ETH
Eidgenössische Technische Hochschule Zürich
Swiss Federal Institute of Technology Zurich

Seminar for Applied Mathematics SAM

Asymptotic Approximation of high order Wavepackets

R. Bourquin and V. Gradinaru

Research Report No. 2016-52
December 2016

Seminar für Angewandte Mathematik
Eidgenössische Technische Hochschule
CH-8092 Zürich
Switzerland

Funding SNF: 140688

Asymptotic Approximation of high order Wavepackets

R. Bourquin and V. Gradinaru

December 1, 2016

Abstract

We demonstrate and analyze the failure of the three-term recursion on the evaluation of Hermite functions for important parameter and argument values. Asymptotic expansions inspire a solution to this problem. We explicitly develop the necessary fomulae in detail and implement an algorithm realizing this solution. The result is applicable to a wide range of input parameter values. The main goal is now an application to Hagedorn wavepackets in one dimension. We can improve the robustness of wavepacket based spectral methods as it becomes possible to evaluate wavepackets of much higher order. The simple example of an overlap matrix computation is shown where we can get rid of any erratic behavior.

1 Motivation

The three term recursion for the Hermite function $h_n(x)$ breaks down for large values of n. This is caused by the finite discrete nature of floating point numbers. There is a limit value $x = \sqrt{2\log(2^{1075})} \approx 38.60397$ (for floating point numbers represented by 64 bits) such that $\exp(-\frac{x^2}{2})$ yields the smallest (denormal) floating point number 2^{-1074}. For any x larger than this limiting value, the floating point evaluation of $h_0(x)$, which is a Gaussian, underflows. The result becomes 0 which propagates up through all the recursion steps until it becomes visible for a large enough index n, when the function h_n is not approximately zero anymore. The Hermite function $h_n(x)$ has for $n > 700$ non-negligible values in the range around that limit value as shown in Figure 1.
Since the Hagedorn wavepackets can be written in terms of Hermite functions this directly limits our ability to work with wavepackets of high order and in turn bounds the maximal basis size for any method based on Hagedorn wavepackets. This problem has been observed before and there are some solutions proposed, for example a stabilized version of the recursion in the appendix of [3] which is however not without its own problems. The main algorithm there for evaluation of Hermite functions is based on quadrature of contour integrals and the evaluation procedure is in general $\mathcal{O}(\sqrt{n})$. We will take a different approach and use asymptotic expansions finally arriving at an $\mathcal{O}(1)$ algorithm suitable for $n > 100$.

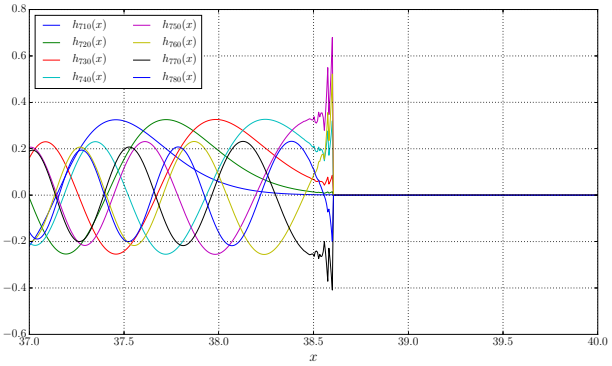

Figure 1: Breakdown of the Hermite function three term recursion for large n.

2 Hagedorn Wavepackets

In one dimension the Hagedorn wavepacket ϕ_k of order k is written as:

$$\begin{aligned}\phi_k(x) = \left(\pi\varepsilon^2\right)^{-\frac{1}{4}} 2^{-\frac{k}{2}} \left(k!\right)^{-\frac{1}{2}} Q^{-\frac{k+1}{2}} \overline{Q}^{\frac{k}{2}} \cdot H_k\left(\varepsilon^{-1}|Q|^{-1}\left(x-q\right)\right) \\ \cdot \exp\left(\frac{\imath}{2\varepsilon^2} P Q^{-1}\left(x-q\right)^2 + \frac{\imath}{\varepsilon^2} p\left(x-q\right)\right)\end{aligned} \tag{1}$$

where $\Pi = \{q, p, Q, P\}$ and ε are the usual parameters. H_k is the Hermite polynomial, so the one-dimensional wavepackets are just properly scaled Hermite functions, denoted by h_k. Hence our goal is to efficiently and accurately approximate Hermite functions $h_n(x)$ of large order n for any (real) argument x. The Hagedorn wavepackets form an orthonormal basis of $L^2(R)$ and hence the overlap matrix:

$$\mathbf{M}_{r,c} := \langle \phi_r[\Pi] | \phi_c[\Pi] \rangle \tag{2}$$

will equal the identity matrix. If we compute this matrix for $0 \leq r, c < 1000$ with enough Gauss-Hermite quadrature points, the resulting $\mathbf{M}$ looks like shown in the left panel of Figure 2.

3 Differential Equations for Hermite functions

In the following we reexamine the theory of asymptotic expansions for Hermite functions $h_k(x)$ for large values of the order n as well as the argument x. The fundamental theory was developed by Olver, see for example his book [21] and the selection of his papers [23]. Most important for us is the paper on uniform asymptotic expansions of parabolic cylinder functions [19]. The Hermite functions:

$$h_n(x) = \left(2^n n! \sqrt{\pi}\right)^{-\frac{1}{2}} e^{-\frac{x^2}{2}} H_n(x) \tag{3}$$

satisfy the following second order differential equation:

$$\frac{\mathrm{d}^2 h_n}{\mathrm{d}x^2} + \left(2n + 1 - x^2\right) h_n = 0\,. \tag{4}$$

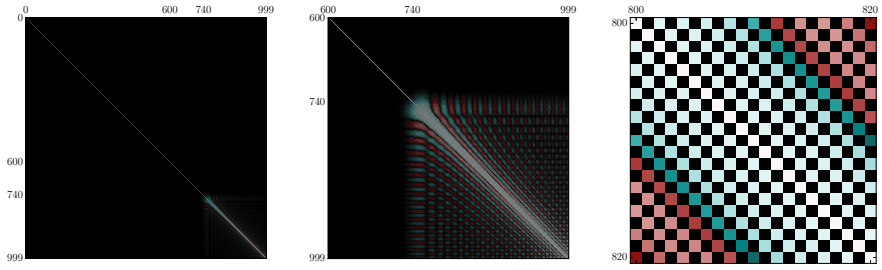

Figure 2: Plot of the overlap matrix $\mathbf{M}_{r,c} := \langle \phi_r | \phi_c \rangle$. Since the wavepackets form an orthonormal basis set, this should give the identity matrix. In the left panel, the full matrix for $0 \leq r, c < 1000$ is shown and there appears an erroneous block in the bottom right corner. The middle panel zooms in to that range, where we can see the main diagonal and the structure of this block. The right panel shows an even larger zoom to the range $800 \leq r, c \leq 820$, half of the elements are non-zero and the maximal in magnitude entry inside this slice is about 0.8244, so not even the elements on the diagonal stay 1 as they should.

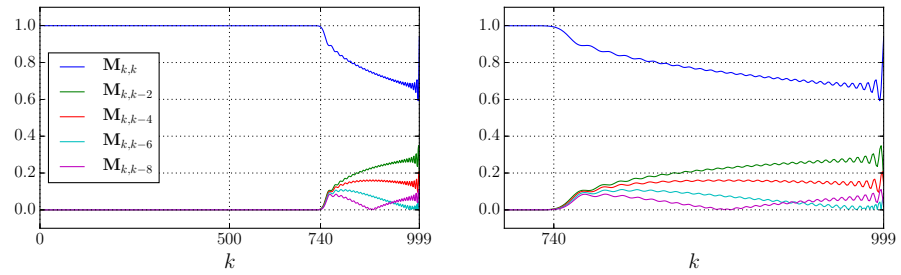

Figure 3: Diagonal and selected off-diagonal elements of the matrix $\mathbf{M}$. These plots show more clearly the large errors introduced into the matrix as mentioned in the caption to Figure 2.

This differential equation is clearly just a special case of the following one:

$$\frac{\mathrm{d}^2 w}{\mathrm{d}x^2} + \left(ax^2 + bx + c\right) w = 0 \tag{5}$$

with $a = -1$, $b = 0$ and $c = 2n + 1$, defining the so called *parabolic cylinder functions*. By completion of the square we can rewrite this as:

$$\frac{\mathrm{d}^2 w}{\mathrm{d}x^2} - \left(\frac{1}{4}x^2 + a\right) w = 0\,. \tag{6}$$

In that case, a pair of independent solutions is given by $U(a, x)$ and $V(a, x)$. More details are given in [1], section 12.2. The connection to the solution of our original problem, the Hermite differential equation, can be established by yet another rewrite. With $\nu = -\frac{1}{2} - a$ we find:

$$\frac{\mathrm{d}^2 w}{\mathrm{d}x^2} + \left(\nu + \frac{1}{2} - \frac{1}{4}x^2\right) w = 0 \tag{7}$$

where one solution $D_\nu(x)$ is called the Whittaker function and obviously:

$$D_\nu(x) = U(-\frac{1}{2} - \nu, x)\,. \tag{8}$$

On the other hand, for the Hermite functions $h_n(x)$ it holds that:

$$D_n(x) = (n!\sqrt{\pi})^{\frac{1}{2}} h_n\left(\frac{x}{\sqrt{2}}\right) \tag{9}$$

and hence:

$$h_n(x) = \left(n!\sqrt{\pi}\right)^{-\frac{1}{2}} D_n(\sqrt{2}x)\,. \tag{10}$$

Finally we get for the Hermite function:

$$h_n(x) = \left(n!\sqrt{\pi}\right)^{-\frac{1}{2}} U(-\frac{1}{2} - n, \sqrt{2}x)\,. \tag{11}$$

With that result is is sufficient to concentrate on asymptotic expansions for $U(a, x)$. These expansions were studied long ago from a theoretical point of view. More recently Temme focused also on the numerical aspects [31, 29]. The usage of parabolic cylinder functions has been studied in a variety of papers [13, 20, 24, 28, 30] by many different researchers.

4 Asymptotic expansion of Hermite functions

In this section we concentrate on the asymptotic expansions for the function $U(a, x)$. By using formula (11) we can in the end construct the expansions for $h_n(x)$. The Hermite functions have a so called *turning point* at $x = \sqrt{2n+1}$ where the oscillatory behavior changes to exponential decay. To get an expansion valid for both regions and also including this transition region we have to use Airy functions which share this feature of changing behavior. The family of Airy functions is well known, in short the functions $\mathrm{Ai}(x)$ and $\mathrm{Bi}(x)$ are solutions of the following second order linear ordinary differential equation with polynomial coefficients:

$$y''(x) - x\,y(x) = 0 \tag{12}$$

and many of their properties are summarized in the book by Vallée and Soares [34]. Another approach to the expansion of Hermite polynomials is given in [35] with some emphasis on the turning point issues. The broader topic of Airy-type expansions are treated for example in [4, 31] and as part of the chapter on *Uniform Asymptotic Expansions* in the classical book [10].
With $\mu := \sqrt{2n+1}$ we can rescale the position variable $t := \frac{x}{\mu}$ and rewrite:

$$U\left(-\frac{1}{2} - n, \sqrt{2}x\right) = U\left(-\frac{1}{2}\mu^2, \sqrt{2}x\right) = U\left(-\frac{1}{2}\mu^2, \sqrt{2}\mu t\right)\,. \tag{13}$$

The two turning points are now located at $t = \pm 1$. For large values of n it is possible to find asymptotic expansions valid in the range $-1 < t \leq \infty$. Since for $n \in \mathbb{N}_0$ it holds that:

$$U\left(-\frac{1}{2} - n, -x\right) = (-1)^n\, U\left(-\frac{1}{2} - n, x\right) \tag{14}$$

we can concentrate entirely on the range $0 \leq x \leq \infty$. Coming now to the central part, the asymptotic expansion:

$$U\left(-\frac{1}{2}\mu^2, \mu t\sqrt{2}\right) \sim$$
$$2\pi^{\frac{1}{2}}\mu^{\frac{1}{3}} g(\mu)\phi(\zeta)\left(\mathrm{Ai}\left(\mu^{\frac{4}{3}}\zeta\right)\sum_{s=0}^{\infty}\frac{A_s(\zeta)}{\mu^{4s}} + \frac{\mathrm{Ai}'\left(\mu^{\frac{4}{3}}\zeta\right)}{\mu^{\frac{8}{3}}}\sum_{s=0}^{\infty}\frac{B_s(\zeta)}{\mu^{4s}}\right) \quad (15)$$

is given in terms of the Airy function $\mathrm{Ai}(x)$ and its derivative $\mathrm{Ai}'(x)$. The formula holds for $|\mu| \to \infty$ with $-\pi < \arg\mu < \pi$ and uniformly with respect to t in some domain of the complex plane. The exact details can be found in [19] and are not relevant for us as we are interested in a very specific simple case. The series converges extremely fast and we can truncate both sums already after three terms each. The use of this excellent expansion for the approximation of Hermite polynomials was hinted by a recent algorithm showing fast computation of Gauss-Hermite quadrature nodes [33]. We implemented this algorithm in the world-wide used package SciPy [14] where it since has become the standard for computing Gauss-Hermite rules of order $n > 150$ up to several thousand points by the function `h_roots`. In the following we will introduce all the other parts of this central formula step by step.

4.1 Series Coefficients

We will first concentrate on the computation of the series coefficients A_s and B_s, which are given by the finite sums:

$$\begin{aligned} A_s(\zeta) &= \zeta^{-3s}\sum_{m=0}^{2s}\beta_m\,\phi(\zeta)^{6(2s-m)}\,u_{2s-m}(t) \\ B_s(\zeta) &= -\zeta^{-3s-2}\sum_{m=0}^{2s+1}\alpha_m\,\phi(\zeta)^{6(2s-m+1)}\,u_{2s-m+1}(t) \end{aligned} \quad (16)$$

where we find new sets of real-valued parameters α_m and β_m. They can be computed easily in closed form:

$$\alpha_0 = 1 \quad (17)$$
$$\alpha_m = \frac{\prod_{j=0}^{2m-1}2m+1+2j}{m!144^m}\,. \quad (18)$$

The first five values are explicitly:

$$\alpha_0 = 1 \quad \alpha_1 = \frac{5}{48} \quad \alpha_2 = \frac{385}{4608} \quad \alpha_3 = \frac{85085}{663552} \quad \alpha_4 = \frac{37182145}{127401984}\,. \quad (19)$$

For the β_m we have:

$$\beta_m = -\frac{6m+1}{6m-1}\alpha_m \quad (20)$$

and again the first five values are:

$$\beta_0 = 1 \quad \beta_1 = -\frac{7}{48} \quad \beta_2 = -\frac{455}{4608} \quad \beta_3 = -\frac{95095}{663552} \quad \beta_4 = -\frac{40415375}{127401984}\,. \quad (21)$$

Beside these raw numbers there are the functions $u_s(t)$ which are polynomials in t of degree $3s$ for odd s and $3s-2$ for even s larger or equal to 2. These polynomials $u_s(t)$ satisfy the following differential equation:

$$(t^2-1)u_s'(t) - 3st\,u_s(t) = r_{s-1}(t)\,. \tag{22}$$

If we know the remainder term $r_{s-1}(t)$ we can compute $u_s(t)$ by solving this first order ordinary differential equation. The remainder itself is given by another difference-differential equation:

$$r_s(t) = \frac{3t^2+2}{8}u_s(t) - \frac{3(s+1)t}{2}r_{s-1}(t) + \frac{t^2-1}{2}r_{s-1}'(t) \tag{23}$$

in terms of u_s and the previous remainder r_{s-1} and its derivative r_{s-1}'. The computation of these polynomials can then be done recursively if we take $r_{-1}(t) \equiv 0$ as shown in Figure 4. This computation yields one after the other the polynomials:

$$\begin{aligned}
u_0(t) &= 1\\
u_1(t) &= \frac{t^3}{24} - \frac{t}{4}\\
u_2(t) &= -\frac{t^4}{128} + \frac{83t^2}{384} + \frac{145}{1152}\\
u_3(t) &= -\frac{2021t^9}{207360} + \frac{2021t^7}{46080} - \frac{3143t^5}{46080} - \frac{10133t^3}{27648} - \frac{2881t}{4608}
\end{aligned} \tag{24}$$

and the corresponding remainders:

$$\begin{aligned}
r_{-1}(t) &= 0\\
r_0(t) &= \frac{3t^2}{8} + \frac{1}{4}\\
r_1(t) &= \frac{t^5}{64} - \frac{5t^3}{6} - \frac{19t}{16}\\
r_2(t) &= -\frac{35t^6}{1024} + \frac{2601t^4}{1024} + \frac{18743t^2}{3072} + \frac{2881}{4608}\\
r_3(t) &= -\frac{2021t^{11}}{552960} + \frac{46483t^9}{3317760} + \frac{32413t^7}{368640} - \frac{3764591t^5}{368640} - \frac{1985809t^3}{55296} - \frac{184483t}{18432}\,.
\end{aligned}$$

Both, polynomials and remainders are plotted in Figure 5. We can also write a direct formula for the closely related functions $\tilde{u}_s(t)$:

$$\tilde{u}_s(t) = \frac{1}{2}\frac{1}{\sqrt{t^2-1}}\frac{\mathrm{d}\tilde{u}_{s-1}(t)}{\mathrm{d}t} + \frac{1}{8}\int \frac{3t^2+2}{(t^2-1)^{\frac{5}{2}}}\tilde{u}_{s-1}(t)\mathrm{d}t \tag{25}$$

with $\tilde{u}_0(t) = 1$. The polynomials $u_s(t)$ are then obtained from these functions by the transformation:

$$u_s(t) = \left(t^2-1\right)^{\frac{3s}{2}}\,\tilde{u}_s(t)\,. \tag{26}$$

It is not obvious that the $u_s(t)$ are indeed polynomials. More details are given by Olver in [19], formula 4.6. We defer the explanation of ζ and $\phi(\zeta)$ from (16) to section 4.3.

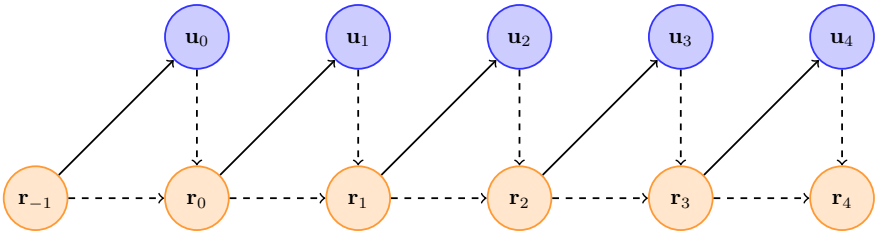

Figure 4: Recursive computation of the polynomials $u_s(t)$ from the remainders $r_s(t)$. The solid arrows represent use of formula (22) and the dashed arrows show the dependency for updating the $r_s(t)$ according to (23). We start the procedure by using the initial value $r_{-1} \equiv 0$.

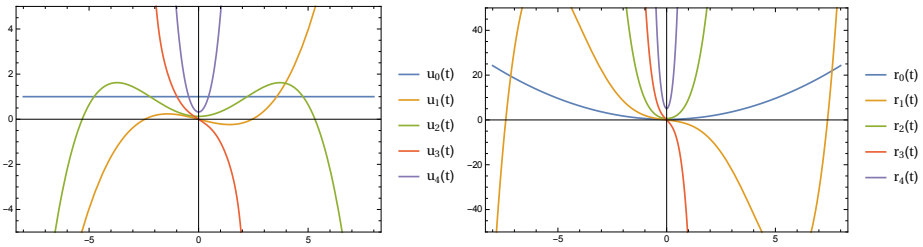

Figure 5: The polynomials $u_s(t)$ (left) and $r_s(t)$ (right). Note the symmetries.

4.2 The Prefactor in $\mathcal{O}(1)$

Let us look at the prefactors of the above expansion (15) in more detail. Besides some numbers we have the functions $g(\mu)$ and $\phi(\zeta)$. We now examine the first function for which another series expansion can be given, see for example equation 12.10.14 in the Digital Library of Mathematical Functions [1]. It holds:

$$g(\mu) \sim h(\mu)s(\mu) \tag{27}$$

where:

$$h(\mu) = 2^{-\frac{1}{4}\mu^2-\frac{1}{4}} e^{-\frac{1}{4}\mu^2} \mu^{\frac{1}{2}\mu^2-\frac{1}{2}} \tag{28}$$

and:

$$s(\mu) = 1 + \frac{1}{2}\sum_{s=1}^{\infty} \frac{\gamma_s}{(\frac{1}{2}\mu^2)^s} \tag{29}$$

with the first few coefficients γ_s being:

$$\gamma_0 = 1 \quad \gamma_1 = -\frac{1}{24} \quad \gamma_2 = \frac{1}{1152} \quad \gamma_3 = \frac{1003}{414720} \quad \gamma_4 = -\frac{4027}{39813120}\,. \tag{30}$$

These values themselves arise from the series expansion:

$$\Gamma\left(\frac{1}{2}+z\right) \sim \sqrt{2\pi} e^{-z} z^z \sum_{s=0}^{\infty} \frac{\gamma_s}{z^s} \tag{31}$$

and can be computed easily on demand.

We gather all the pure numerical factors from (11) and from (15) and also include $h(\mu)$ but not $s(\mu)$ into a common large prefactor τ:

$$\begin{aligned}\tau(n) &:= \left(n!\sqrt{\pi}\right)^{-\frac{1}{2}} 2\pi^{\frac{1}{2}}\mu^{\frac{1}{3}}h(\mu) \\ &= (n!)^{-\frac{1}{2}}\,\pi^{\frac{1}{4}}2^{-\frac{1}{4}\mu^2+\frac{3}{4}}e^{-\frac{1}{4}\mu^2}\mu^{\frac{1}{2}\mu^2-\frac{1}{6}}\end{aligned} \tag{32}$$

and $\tilde{\tau}(n) := \tau(n)s(\mu)$. Practical computation of this factor τ is difficult mostly for the reason that the value of μ which can be quite large appears in the exponents. Also there is the factorial term $n!$ in the denominator. Together these large values cancel to yield reasonable ranges for $\tau(n)$ of $\mathcal{O}(1)$. Figure 6a shows the function $\tau(n)$ for $n \in [0, 1000]$ computed by extended precision arithmetic. Even if the plot might suggest otherwise, it holds that:

$$\tau(0) = \sqrt{2}\sqrt[4]{\frac{\pi}{e}} \approx 1.4663203 \quad \text{and} \quad \lim_{n\to\infty}\tau(n) = 0 \tag{33}$$

which can be checked by explicit computation.

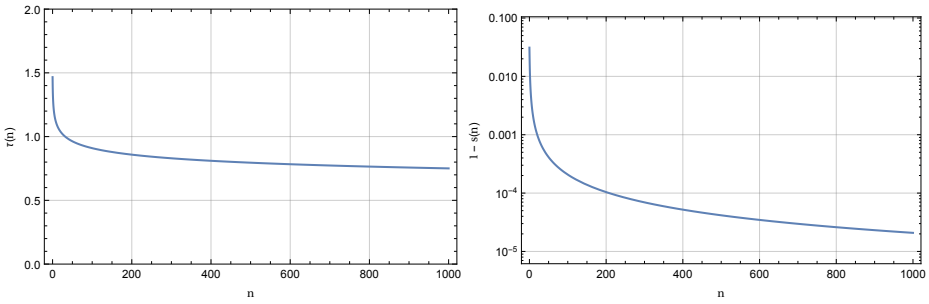

(a) (b)

Figure 6: Plot of the function $\tau(n)$ (left) computed by extended arithmetic over the range $n \in [0, 1000]$. The right plot shows the value of $1 - s(n)$ for $n \in [0, 1000]$ in a logarithmic plot. Over the whole range of n but even more for the larger n the function $s(n)$ is almost equal to one.

If we just naively evaluate the symbolic expression for $\tau(n)$ or $\tilde{\tau}(n)$ respectively the numerics breaks down just after $n = 170$ already. This is shown by the red curve in Figure 7a.
Let us define the approximation $\tilde{h}_n^{\text{asy}}(x)$ to $h_n(x)$ obtained from the formula (15) by taking just the part in large brakets and $\phi(\zeta)$. The three term recursion for the Hermite function $h_n(x)$ can be evaluated in forward mode for any n as long as x is small enough to avoid the problems mentioned in the beginning. Since the prefactor $\tilde{\tau}$ is just a scalar factor independent of x we can use the following trick:

$$\tilde{\tau}(n) = \frac{h_n(x_0)}{\tilde{h}_n^{\text{asy}}(x_0)} \tag{34}$$

where we choose a fixed evaluation point x_0. The question is how to choose this point. A first idea is to fix $x_0 = 1$. Another possibility is to choose $x_0 = 0$ for even n and $x_0 = 1$ for odd n. Both methods are unstable for some values of n because there are Hermite functions which have a zero in the vicinity of the

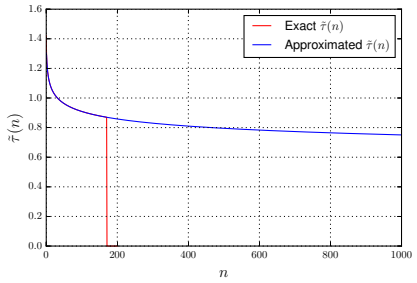

(a) Exact value of the $\tau(n)$ parameter and the numerical approximation.

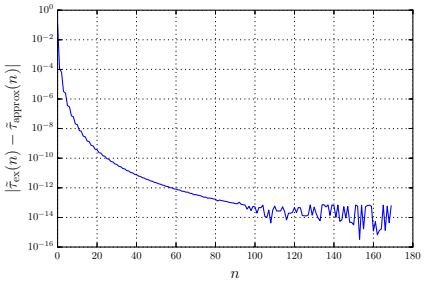

(b) Difference of the exact value and the numerical approximation.

Figure 7: The prefactor $\tilde{\tau}(n)$. Computation by the exact formula breaks down even before $n = 200$ while the numerical approximation can be applied to much larger values.

chosen x_0. In order to obtain a robust evaluation we can choose x_0 as the first non-negative maximum of the Hermite function h_n. This point can be found as the zero of the derivative:

$$0 \stackrel{!}{=} h_n'(x_0) = \sqrt{\frac{n}{2}} h_{n-1}(x_0) - \sqrt{\frac{n+1}{2}} h_{n+1}(x_0) \tag{35}$$

which itself can be computed by a variant of the recursion relation. Instead of using the exact zero which is not straight forward to compute we use the approximate value implicitly specified by:

$$0 = h_{n+1}(x_0) \tag{36}$$

which is close enough. This value can be computed very efficiently in $\mathcal{O}(1)$ by the algorithm presented in [32]. Figure 8 shows the maximal absolute approximation error of $h_n^{\text{asy}}(x)$ compared to $h_n(x)$ for x in the range $\pm\frac{3}{2}\sqrt{2n+1}$. The blue curve in Figure 7 shows the values of $\tilde{\tau}$ obtained by this approach and the Figure 7b shows the difference to the evaluation of the symbolic formula. If we keep in mind that we deal with an asymptotic approximation and that we will use it for say $n > 100$ this all fit together well.
Note that this method has also a drawback from the efficiency point of view as the computation of $\tilde{\tau}$ becomes $\mathcal{O}(n)$ because we have to use the recursion relation. We present a better solution. As can be seen in Figure 6b the $s(n)$ part of $\tilde{\tau}(n)$ is extremely tame. We focus on the $\tau(n)$ part from equation (32). First we look at the term $n! = \Gamma(n+1)$. The gamma function is an opaque block we can not handle in this form. Hence we use the following modern approximation for the gamma function:

$$\Gamma(\xi) \approx \sqrt{\frac{2\pi}{\xi}} \left(\frac{1}{e} \left(\xi + \frac{1}{12\xi - \frac{1}{10\xi}} \right) \right)^{\xi}. \tag{37}$$

which is formula 4.1 in [18] and therein referred as *closed approximation*[1]. We

[1]Even more accurate approximations to $\Gamma(x)$ like *Nemes-6*, *Nemes-8* or methods proposed in [17] could be used. Some of these ideas go back to [27].

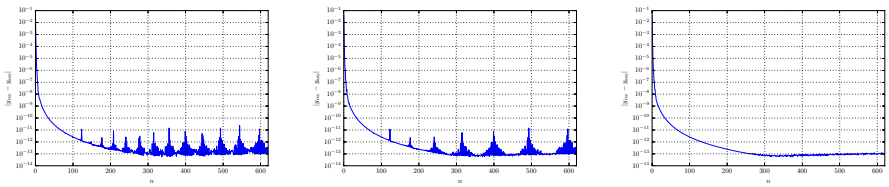

(a) Computing the prefactor always at the point $x_0 = 1$.

(b) Computing the prefactor at $x_0 = 0$ if n is even and at $x_0 = 1$ if n is odd.

(c) Computing the prefactor at the smallest non-negative maximum.

Figure 8: Maximal absolute approximation error. For values of n larger than 600 the reference solution computed by recursion starts to fail. The peaks in the first figures are caused by zeros of h_n in the vicinity of the chosen x_0.

define the abbreviation:

$$\delta := (n+1) + \frac{1}{12(n+1) - \frac{1}{10(n+1)}}\,. \tag{38}$$

Next we get:

$$\begin{aligned}
\Gamma(n+1) &\approx \sqrt{\frac{2\pi}{n+1}} \left(\frac{\delta}{e}\right)^{n+1} \\
\sqrt{\Gamma(n+1)} &\approx \left(\frac{2\pi}{n+1}\right)^{\frac{1}{4}} e^{-\frac{n+1}{2}} \delta^{\frac{n+1}{2}} \\
\frac{1}{\sqrt{\Gamma(n+1)}} &\approx \left(\frac{n+1}{2\pi}\right)^{\frac{1}{4}} e^{\frac{n+1}{2}} \delta^{-\frac{n+1}{2}}\,.
\end{aligned} \tag{39}$$

We plug this into the formula for the factor $\tau(n)$ and write all the factors as exponentials as follows:

$$\begin{aligned}
\tau(n) &\approx \tau^{\text{approx}}(n) \\
&= \left(\frac{n+1}{2\pi}\right)^{\frac{1}{4}} e^{\frac{n+1}{2}} \delta^{-\frac{n+1}{2}} \pi^{\frac{1}{4}} 2^{-\frac{1}{4}\mu^2+\frac{3}{4}} e^{-\frac{1}{4}\mu^2} \mu^{\frac{1}{2}\mu^2-\frac{1}{6}} \\
&= (n+1)^{\frac{1}{4}} e^{\frac{n+1}{2}} \delta^{-\frac{n+1}{2}} 2^{-\frac{1}{4}\mu^2+\frac{1}{2}} e^{-\frac{1}{4}\mu^2} \mu^{\frac{1}{2}\mu^2-\frac{1}{6}} \\
&= e^{\log(n+1)\frac{1}{4}} e^{\frac{n+1}{2}} e^{-\log(\delta)\frac{n+1}{2}} e^{-\log(2)\left(\frac{1}{4}\mu^2+\frac{1}{2}\right)} e^{-\frac{1}{4}\mu^2} e^{\log(\mu)\left(\frac{1}{2}\mu^2-\frac{1}{6}\right)}
\end{aligned} \tag{40}$$

If we collect and group all the factors this results in:

$$\begin{aligned}
\tau^{\text{approx}}(n) = \exp\Bigg(\frac{1}{4} - \left(\frac{n}{2} - \frac{1}{4}\right)\log(2) - \frac{(n+1)}{2}\log(\delta) \\
+ \left(n + \frac{1}{3}\right)\log(\sqrt{2n+1}) + \frac{1}{4}\log(n+1)\Bigg)
\end{aligned} \tag{41}$$

and we can write the approximate prefactor $\tau^{\text{approx}}(n)$ as a single exponential. Again we have:

$$\tau^{\text{approx}}(0) = \sqrt{\frac{119}{129}}\sqrt[4]{2e} \approx 1.4665935 \quad \text{and} \quad \lim_{n\to\infty} \tau^{\text{approx}}(n) = 0\,. \tag{42}$$

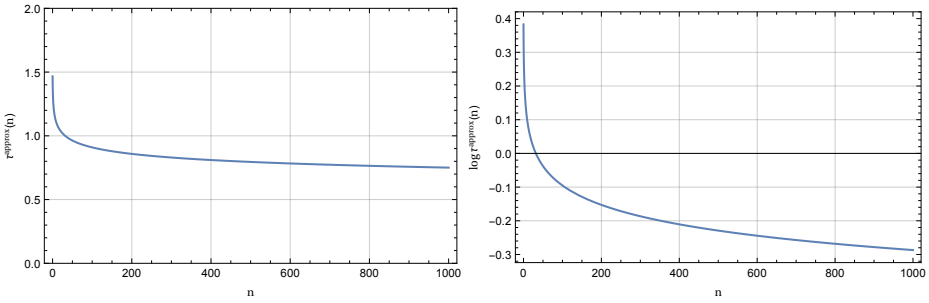

(a) (b)

Figure 9: Plot of the function $\tau^{\text{approx}}(n)$ (left) over the range $n \in [0, 1000]$. The right plot shows the exponent from equation (41) for $n \in [0, 1000]$.

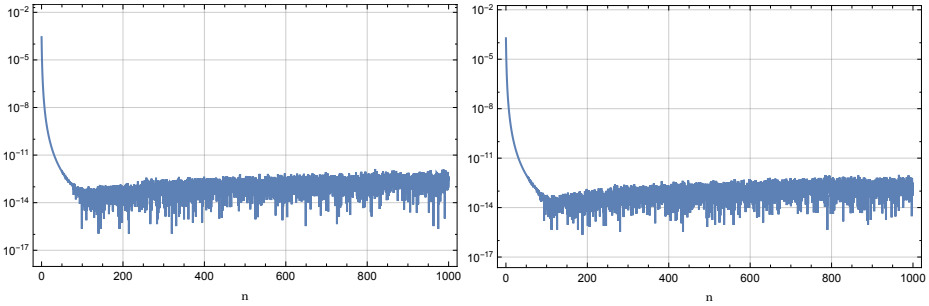

(a) (b)

Figure 10: Absolute error (left) and relative error (right) of the approximation $\tau^{\text{approx}}(n)$ over the range $n \in [0, 1000]$.

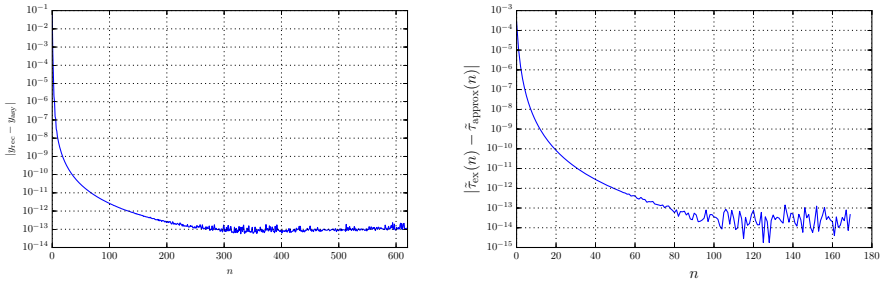

(a) Computing the prefactor via gamma function expansion.

(b) Difference of the exact value and the numerical approximation.

Figure 11: Maximal absolute approximation error (left) while using the approximate prefactor. The prefactor $\tilde{\tau}^{\text{approx}}(n)$ (right).

4.3 The middle part

The final part missing in the asymptotic expansion is the function $\phi(\zeta)$. It is defined as:

$$\phi(\zeta) := \left(\frac{\zeta}{t^2-1}\right)^{\frac{1}{4}} \tag{43}$$

Notice that exactly at the turning points $t = \pm 1$ this formula will yield a division by zero. This causes some difficulties later but we are able to overcome those. Nested inside the above expression for ϕ is ζ which itself is a function of t. This function is implicitly defined by the following two expressions:

$$\frac{2}{3}(-\zeta)^{\frac{3}{2}} = \eta \qquad -1 < t \leq 1 \tag{44}$$

$$\frac{2}{3}\zeta^{\frac{3}{2}} = \xi \qquad 1 \leq t \leq \infty \tag{45}$$

It is important to note that $\zeta(1)$ is analytic. This property will later resolve all issues at this special point. The right hand sides are:

$$\begin{aligned} \eta(t) &= -\frac{1}{2}t\sqrt{1-t^2} + \frac{1}{2}\imath \log\left(t - \imath\sqrt{1-t^2}\right) \\ \xi(t) &= \frac{1}{2}t\sqrt{t^2-1} - \frac{1}{2}\log\left(t + \sqrt{t^2-1}\right) \end{aligned} \tag{46}$$

and shown in Figure 12. Obviously they are both zero at $t = 1$. Next we can compute $\zeta(t)$ and get:

$$\zeta(t) = \begin{cases} -\left(\frac{3\eta(t)}{2}\right)^{\frac{2}{3}} & t < 1 \\ 0 & t = 1 \\ \left(\frac{3\xi(t)}{2}\right)^{\frac{2}{3}} & t > 1 \end{cases} \tag{47}$$

as shown in Figure 13. In turn we resolve $\phi(\zeta)$ and get:

$$\phi(\zeta(t)) = \left(\frac{\zeta(t)}{t^2-1}\right)^{\frac{1}{4}}. \tag{48}$$

At $t = 1$ we see an indefinite expression ϕ however the limit from both sides exists and the function is continuous. If we use this whole machinery to compute asymptotic approximations, the results look as depicted in Figure 15 for the Hermite function $h_{400}(x)$.

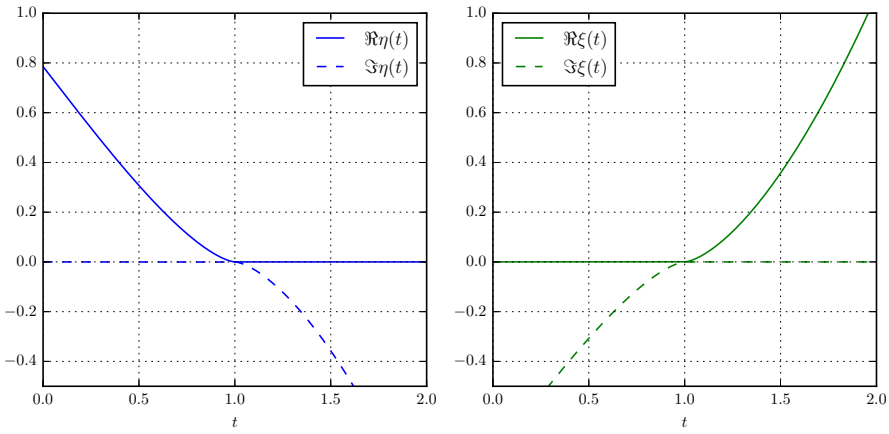

Figure 12: The functions $\eta(t)$ and $\xi(t)$.

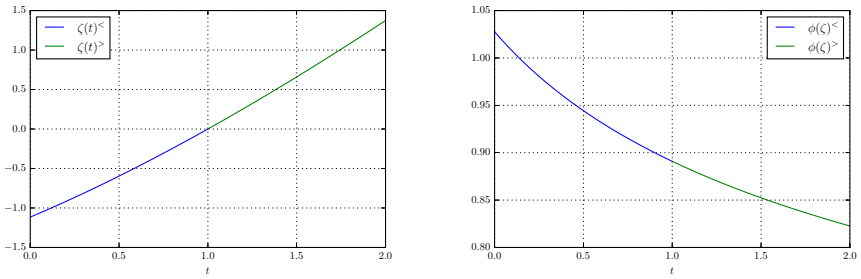

Figure 13: The functions $\zeta(t)$ and $\phi(\zeta)$.

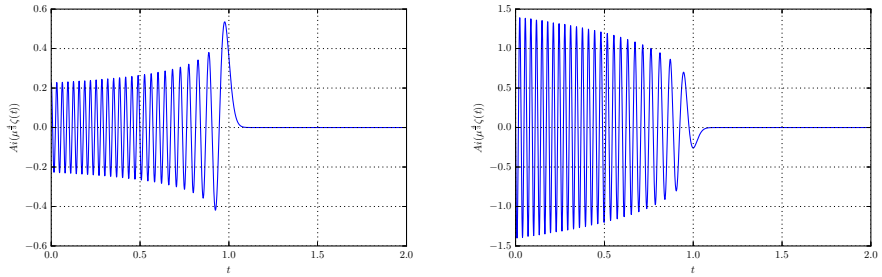

Figure 14: The functions $\mathrm{Ai}(\mu^{4/3}\zeta(t))$ and $\mathrm{Ai}'(\mu^{4/3}\zeta(t))$.

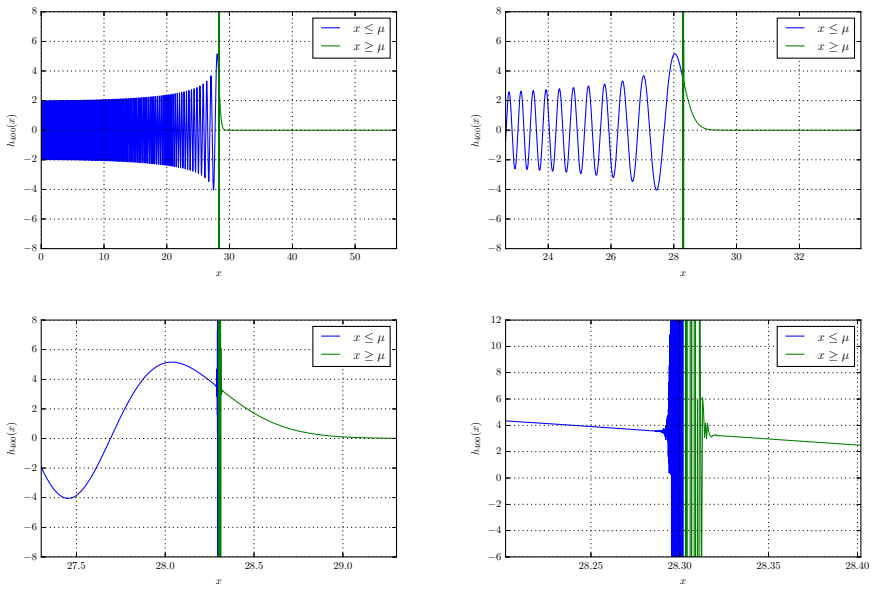

Figure 15: Asymptotic approximation of $h_{400}(x)$. The plots zoom in around the turning point $\mu = \sqrt{2n+1}$, in this case $\mu = \sqrt{801} \approx 28.3$. We find a strongly localized blow up at this point.

4.4 Patching the turning point

As we can see in Figure 15, special care needs to be taken for values in a close neighborhood around the turning point at $t = 1$ or $x = \mu$ respectively. The exact values at the point μ can be computed from the formal sums for $H_n(x)$:

$$h_n(\mu) = \begin{cases} \frac{\imath^n\, 2^{-\frac{n}{2}}\, \sqrt{n!}\, e^{-n-\frac{1}{2}}}{\sqrt[4]{\pi}\,\Gamma\left(\frac{n+2}{2}\right)}\, {}_1F_1\left(-\frac{n}{2}; \frac{1}{2} \middle| 2n+1\right) & n \text{ even} \\ \frac{\imath^{n+3}\, 2^{1-\frac{n}{2}}\, \sqrt{(2n+1)}\, \sqrt{n!}\, e^{-n-\frac{1}{2}}}{\sqrt[4]{\pi}\,\Gamma\left(\frac{n+1}{2}\right)}\, {}_1F_1\left(\frac{1}{2}-\frac{n}{2}; \frac{3}{2} \middle| 2n+1\right) & n \text{ odd}\,. \end{cases} \tag{49}$$

The expression (15) derived in the last section has a divergence at this point. There are several subexpressions including terms like $t^2 - 1$ for example in the functions η and ξ which make up ζ as well as in the denominator of the expression for ϕ. However, the function $\zeta(t)$ is analytic at $t = 1$, as shown in [19] and also mentioned in [1], formula 12.10.41. Hence we can compute a series expansion around $t = 1$. Doing this up to third order we find:

$$\zeta(t) = -\frac{311}{350}2^{\frac{1}{3}} + \frac{134}{175}2^{\frac{1}{3}}t + \frac{47}{350}2^{\frac{1}{3}}t^2 - \frac{2}{175}2^{\frac{1}{3}}t^3 + \mathcal{O}(t^4)\,. \tag{50}$$

Next we can insert this into the definition of $\phi(\zeta)$ and again compute a series expansion around $t = 1$. We get:

$$\phi(\zeta(t)) = \frac{16031}{14000}2^{-\frac{1}{6}} - \frac{2843}{14000}2^{-\frac{1}{6}}t + \frac{993}{14000}2^{-\frac{1}{6}}t^2 - \frac{181}{14000}2^{-\frac{1}{6}}t^3 + \mathcal{O}(t^4)\,. \tag{51}$$

Now the process becomes more complicated, as the main ingredients, A_s and B_s, depend on ζ but also directly on t through the polynomials $u_s(t)$. Since the function $\zeta(t)$ in analytic we can invert it around $t = 1$ and find:

$$t(\zeta) = 1 + 2^{-\frac{1}{3}}\zeta - \frac{1}{10}2^{-\frac{2}{3}}\zeta^2 + \frac{11}{350}2^{-\frac{3}{3}}\zeta^3 - \frac{823}{63000}2^{-\frac{4}{3}}\zeta^4 + \frac{150653}{24255000}2^{-\frac{5}{3}}\zeta^5 + \mathcal{O}(\zeta^6)\,.$$

We plug this together with the series expansion for ζ into the definitions from (16). Then we can expand $A_s(\zeta)$ and $B_s(\zeta)$ around $\zeta = 0$. The first three terms of both series up to second order are:

$$\begin{aligned} A_0(\zeta) &= 1 \\ A_1(\zeta) &= -\frac{83}{9600} + \frac{6849}{616000}2^{-\frac{1}{3}}\zeta - \frac{6963757}{591360000}2^{-\frac{2}{3}}\zeta^2 + \mathcal{O}(\zeta^3) \\ A_2(\zeta) &= \frac{164424546127}{26824089600000} - \frac{2268401006387}{190749081600000}2^{-\frac{1}{3}}\zeta + \mathcal{O}(\zeta^2) \end{aligned} \tag{52}$$

and:

$$\begin{aligned} B_0(\zeta) &= -\frac{9}{140}2^{-\frac{2}{3}} + \frac{7}{225}2^{-\frac{3}{3}}\zeta - \frac{1359}{67375}2^{-\frac{4}{3}}\zeta^2 + \mathcal{O}(\zeta^3) \\ B_1(\zeta) &= \frac{6402643}{286720000}2^{-\frac{2}{3}} - \frac{23658594097}{1117670400000}2^{-\frac{3}{3}}\zeta + \frac{533862734809}{23843635200000}2^{-\frac{4}{3}}\zeta^2 + \mathcal{O}(\zeta^3) \\ B_2(\zeta) &= -\frac{2789441829184657}{80114614272000000}2^{-\frac{2}{3}} + \frac{193350809601223663}{4326189170688000000}2^{-\frac{3}{3}}\zeta + \mathcal{O}(\zeta^2)\,. \end{aligned} \tag{53}$$

Finally we just need to assemble all the parts according to formula (15). For the actual implementation we use series expansions up to higher orders than shown here.

All these expansions are accurate only in a region around $t = 1$. The series (4.4) converges for $|\zeta| < (\frac{3\pi}{4})^{\frac{2}{3}}$. We choose $\tau = \varepsilon^{\frac{1}{8}}/\mu$ with ε the machine precision and determine a suitable region where to apply this patch. From some experiments the following region[2] seems to be appropriate:

$$[1 - (3\tau)^{\frac{2}{3}}, 1 + (3\tau)^{\frac{2}{3}}]. \tag{54}$$

The region is also shown in the figures 16 and 17 by vertical magenta lines. Numerical experiments showing the perfect fit of the patch for large n.
This procedure for patching the turning point works fine in practice but is not a nice solution. Maybe one should look at the different approximations shown in [29]. Probably there are better ways to overcome the divergence.

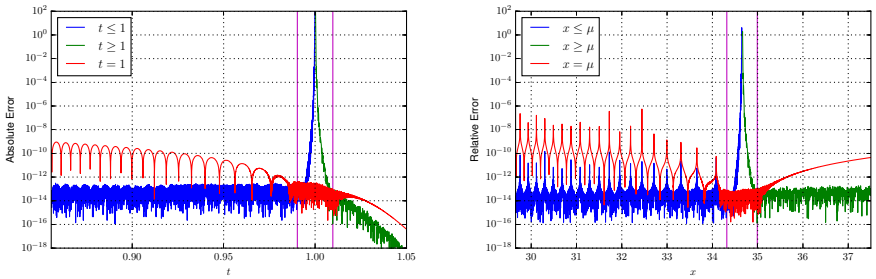

(a) (b)

Figure 16: Absolute (left) and relative (right) error of the patched asymptotic approximation of $h_{600}(x)$ compared to the version obtained via three term recursion.

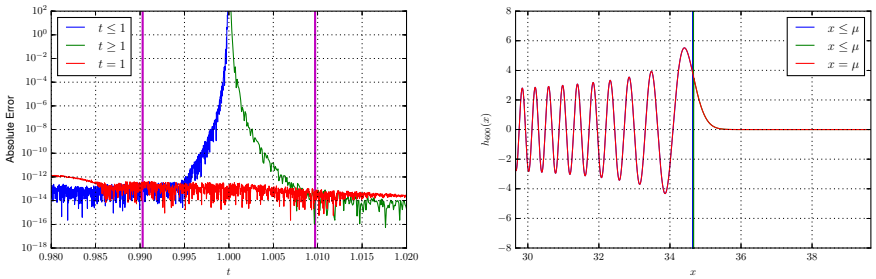

(a) (b)

Figure 17: Left: relative error of the patched asymptotic approximation of $h_{600}(x)$ zoomed in around the turning point. Right: the patched asymptotic approximation of $h_{600}(x)$ having no visible defects.

[2]The series expansion of $\xi(t)$ around $t = 1$ up to second order is: $c = \frac{2}{3}\sqrt{2}(t-1)^{\frac{3}{2}} + \mathcal{O}(t^{\frac{5}{2}})$ and solving this for t we find: $t = 1 + \frac{1}{2}(3c)^{\frac{2}{3}}$ from which we deduce a guess for the region.

4.5 Recapitulation and concrete procedure

Taking a top-down approach, the Hermite function $h_n(x)$ is rewritten in terms of the parabolic cylinder function U by (11). The numerical evaluation of U is done through the asymptotic expansion formula (15). In case x is negative, we apply (14) and hence consider positive values only. This is reflected in the Algorithms 1 and 2.
For general positive values of x the procedure is summarized in the following. We need ζ which we calculate according to its definition (47) which incorporates the two functions ξ and η from (46). These steps are contained within the Algorithms 4 and 5. Next, we compute the coefficients A_s and B_s via (16) wherein we need the values α_i and β_i as given in (19) and (21) and the polynomials from listing (24). The term $\phi(\zeta)$ is formed according to (48). This forms the core and is outlined in Algorithm 6.
Further, we compute the prefactor of (15) including the factors stemming from the transformation (11). The s part inside g is easy and uses (29) with scalars from (30). The remaining terms are then collected in τ as shown in (32) and we plug in the approximation (41) for τ with δ from formula (38), compare also to Algorithm 3.
If the value of x is in the vicinity of the turning point, a region roughly defined by (54) after changing to the t variable, we need a special treatment. The function $\zeta(t)$ is built from a series expansion in t around 1 as shown in (50). Then the coefficients A_s and B_s are computed as series expansions in terms of ζ as presented in (52) and (53). Also the function ϕ is expanded in t like printed in formula (51) and sketched in Algorithm 7.
Note that in the actual code we use longer series expansions of higher degree which are not reproduced here for reasons of brevity.
Working with a variable θ defined implicitly by $t = \cos(\theta)$ in case $t < 1$ and by $t = \cosh(\theta)$ when $t > 1$ rather than with t is beneficial for numerical stability, as explained in [33].
The different parts of this algorithm are split into several function definitions given below. The main entry point is Algorithm 1. The function boundaries are not always aligned with the mathematics because of computational reasons. All parts can easily be vectorized to work with $\underline{x} \in \mathbb{R}^n$ instead of $x \in \mathbb{R}$ as done in our implementation.

Algorithm 1 Hermite evaluation by asymptotic expansion: main entry point

```
procedure HermiteAsy(n, x)
    y := 0                                              ▷ Apply Formula (11)
    if x < 0 then
        y := (−1)^(n mod 2) HermiteAsyPositive(n, −x)   ▷ Formula (14)
    else
        y := HermiteAsyPositive(n, x)
    end if
    τ̃ := GetTau(n)
    return τ̃ y
end procedure
```

Algorithm 2 Dispatch evaluation for positive x values

procedure HERMITEASYPOSITIVE(n, x)
  $\mu := \sqrt{2n+1}$ ▷ Rescale the x value
  $t := \frac{x}{\mu}$
  ▷ Bound the region around the turning point $t = 1$
  $\sigma := \epsilon^{\frac{1}{8}}/\mu$
  $t^- := 1 - (3\sigma)^{\frac{2}{3}}$ ▷ Formula (54)
  $t^+ := 1 + (3\sigma)^{\frac{2}{3}}$
  ▷ Evaluate for each region $[0, t^-) \cup [t^-, t^+] \cup (t^+, \infty)$ separately
  $y := 0$
  if $t < t^-$ **then**
    $y :=$ PBCFASYSMALL(n, t)
  else if $t > t^+$ **then**
    $y :=$ PBCFASYLARGE(n, t)
  else
    $y :=$ PBCFSERIESTURNINGPOINT(n, t)
  end if
  return y
end procedure

Algorithm 3 Compute the scalar prefactor $\tilde{\tau}$

procedure GETTAU(n)
  $\delta := (n+1) + \frac{1}{12(n+1) - \frac{1}{10(n+1)}}$ ▷ Formula (38)
  $\tau^{approx} := \frac{1}{4} - \left(\frac{n}{2} - \frac{1}{4}\right)\log(2) - \frac{(n+1)}{2}\log(\delta) + \left(n + \frac{1}{3}\right)\log(\sqrt{2n+1}) + \frac{1}{4}\log(n+1)$
  ▷ Exponent of Formula (41)
  $s := 1 + \frac{1}{2}\sum_{i=1}^{4} \gamma_i \, (n + \frac{1}{2})^{-i}$ ▷ Formula (29) with (30)
  $\tilde{\tau} := s \exp(\tau^{approx})$
  return $\tilde{\tau}$
end procedure

Algorithm 4 Parabolic cylinder function series helper for $t < 1$

procedure PBCFASYSMALL(n, t)
  $\mu := 2n + 1$
  $\theta := \arccos(t)$ ▷ Numerical trick from [33]
  $s_t := \sin(\theta)$
  $c_t := \cos(\theta)$
  $\eta := \frac{1}{2}\theta - \frac{1}{2}s_t c_t$ ▷ Reformulation of (46)
  $\zeta := -(\frac{3\eta}{2})^{\frac{2}{3}}$ ▷ Formula (47)
  $\phi := (-\frac{\zeta}{s_t^2})^{\frac{1}{4}}$ ▷ Formula (48)
  $y :=$ PBCFSERIES(μ, c_t, ζ, ϕ)
  return y
end procedure

Algorithm 5 Parabolic cylinder function series helper for $t > 1$

procedure PBCFAsyLarge(n, t)
  $\mu := 2n + 1$
  $\theta := \operatorname{arccosh}(t)$ ▷ Numerical trick from [33]
  $s_t := \sinh(\theta)$
  $c_t := \cosh(\theta)$
  $\xi := \frac{1}{2} s_t c_t - \frac{1}{2} \log(s_t + c_t)$ ▷ Reformulation of (46)
  $\zeta := (\frac{3\xi}{2})^{\frac{2}{3}}$ ▷ Formula (47)
  $\phi := (\frac{\zeta}{s_t^2})^{\frac{1}{4}}$ ▷ Formula (48)
  $y :=$ PBCFSeries(μ, c_t, ζ, ϕ)
  return y
end procedure

Algorithm 6 Asymptotic series expansion of parabolic cylinder function U

procedure PBCFSeries(μ, c_t, ζ, ϕ)
  ▷ Coefficients
  $\alpha_0, \ldots, \alpha_5 := \ldots$ ▷ Formula (19) and (21)
  $\beta_0, \ldots, \beta_5 := \ldots$
  ▷ Polynomials
  $u_0(c_t), \ldots, u_5(c_t) := \ldots$ ▷ Formula (24)
  $A_i := \mathrm{Ai}(\mu^{\frac{4}{6}} \zeta)$ ▷ Airy function evaluation
  $Aip := \mathrm{Ai}'(\mu^{\frac{4}{6}} \zeta)$
  ▷ Terms for series of U
  $A_0, \ldots, A_2 := \ldots$ ▷ Formula (16)
  $B_0, \ldots, B_2 := \ldots$
  ▷ Assemble U
  $U := \phi \cdot \left(A_i \cdot (A_0 + \frac{A_1}{\mu^2} + \frac{A_2}{\mu^4}) + \frac{A_{ip}}{\mu^{\frac{8}{6}}} \cdot (B_0 + \frac{B_1}{\mu^2} + \frac{B_2}{\mu^4}) \right)$ ▷ Main part of (15) **return** U
end procedure

Algorithm 7 Asymptotic series expansion of U around the turning point

procedure PBCFSeriesTurningPoint(n, t)
$\mu := 2n + 1$
▷ Series inversion
$\zeta := \ldots$ ▷ Formula (50)
$\phi := \ldots$ ▷ Formula (51)

$A_i := \mathrm{Ai}(\mu^{\frac{4}{6}}\zeta)$ ▷ Airy function evaluation
$Aip := \mathrm{Ai}'(\mu^{\frac{4}{6}}\zeta)$
▷ Terms for series of U
$A_0, \ldots, A_2 := \ldots$ ▷ Formula (52) and (53)
$B_0, \ldots, B_2 := \ldots$
▷ Assemble U
$U := \phi \cdot \left(A_i \cdot (A_0 + \frac{A_1}{\mu^2} + \frac{A_2}{\mu^4}) + \frac{A_{ip}}{\mu^{\frac{8}{6}}} \cdot (B_0 + \frac{B_1}{\mu^2} + \frac{B_2}{\mu^4}) \right)$ ▷ Main part of (15) **return** U
end procedure

5 Numerical Examples

In this section we show a few numerical examples. First we retry on the evaluation of high order Hermite functions as in Figure 1. With the new algorithm in place, we no longer observe these issues as can be seen in Figure 18.

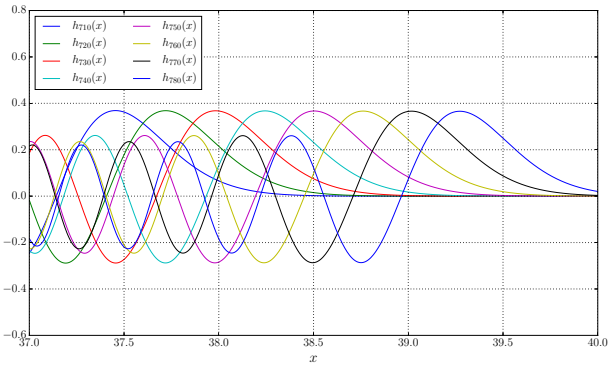

Figure 18: Hermite functions $h_n(x)$ for large n by direct evaluation via the asymptotic expansion. The functions are all complete and without the breakdown at $x \approx 38.6$. Compare this to Figure 1.

The plots in Figure 19 show the absolute and relative error behavior for small n. While even for $n = 1$ the error is smaller than 10^{-3} and hence barely visible, we can achieve good results already for $n = 50$ which is rather small. The errors around the turning point are typically around two orders of magnitude larger in that range of n.
The other plots in Figure 20 show the errors for larger values of n up to the point where we do not have a good reference solution provided by the three term

recursion any longer. We can obtain errors in the order of 10^{-14} over the full range of x values, including the turning points. We almost reach the machine precision.
It is not obvious in which part of the algorithm one should improve to get even smaller error values. Maybe also the reference solution is not accurate enough.

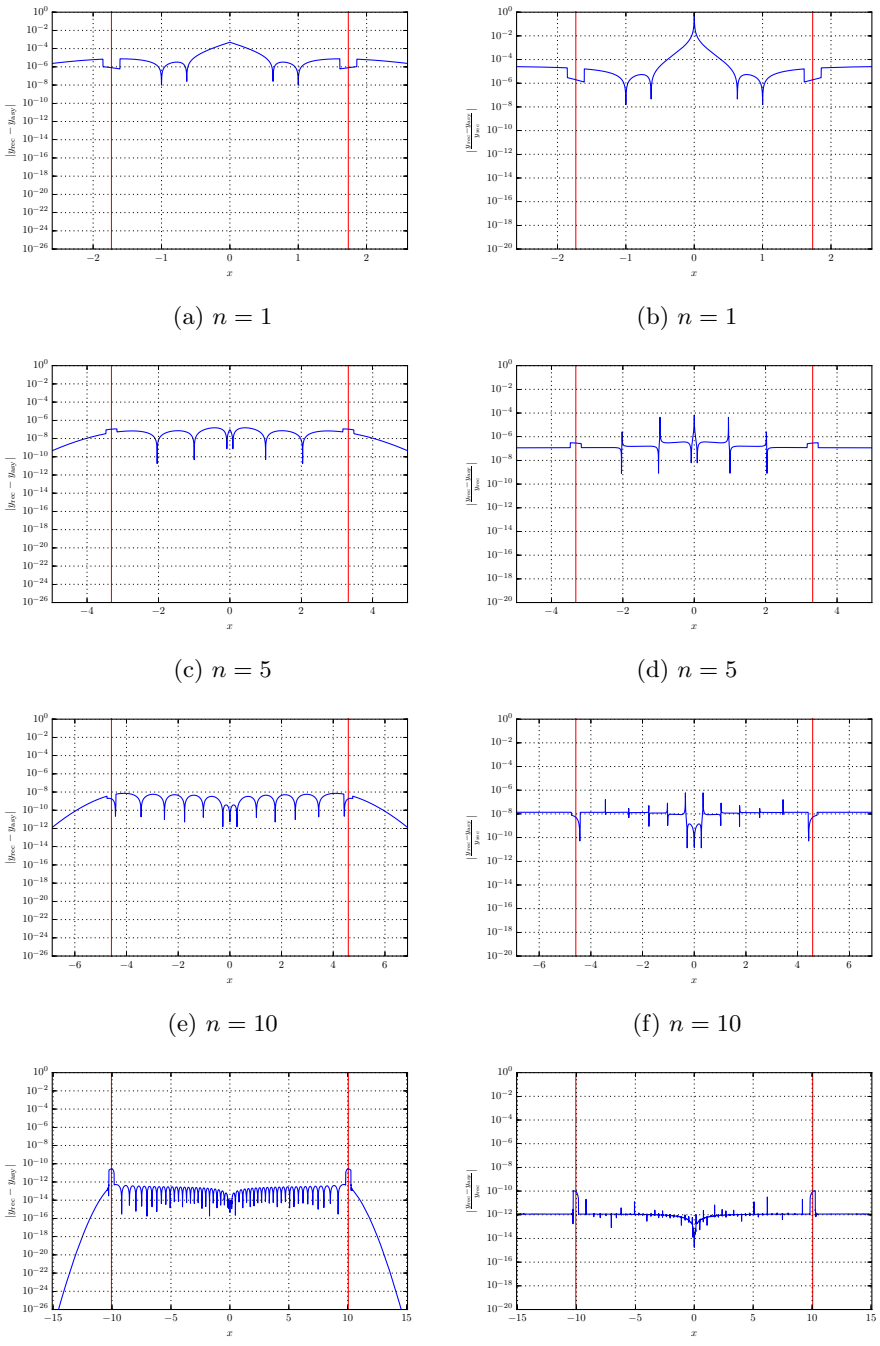

(a) $n = 1$ (b) $n = 1$

(c) $n = 5$ (d) $n = 5$

(e) $n = 10$ (f) $n = 10$

(g) $n = 50$ (h) $n = 50$

Figure 19: Absolute (left column) and relative (right column) error of the asymptotic version compared to the recursive version of the Hermite function $h_n(x)$. The red lines mark the turning point $x = \mu = \pm\sqrt{2n+1}$. Already for very small $n = 50$, the error is about 10^{-12}. Around the turning points the error is about two orders of magnitude larger.

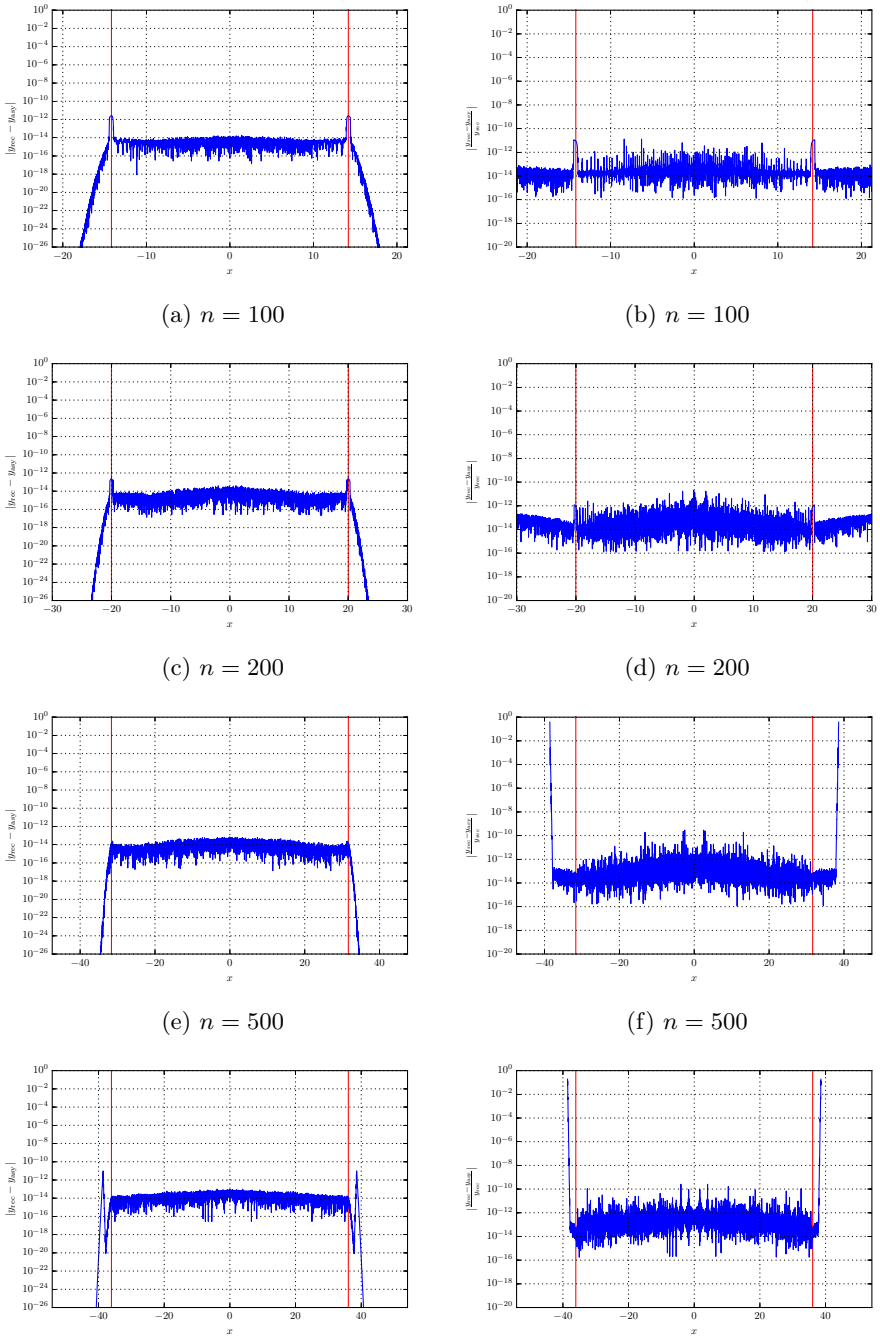

(a) $n = 100$ (b) $n = 100$

(c) $n = 200$ (d) $n = 200$

(e) $n = 500$ (f) $n = 500$

(g) $n = 650$ (h) $n = 650$

Figure 20: Absolute (left column) and relative (right column) error of the asymptotic version compared to the recursive version of the Hermite function $h_n(x)$. The red lines mark the turning point $x = \mu = \pm\sqrt{2n+1}$. For larger n the errors decrease to 10^{-14} which is almost machine precision. Also, the error around the turning points is now of the same order.

6 Transformation of Wavepackets

6.1 One dimensional case

Given a Hagedorn wavepacket $\phi_k[\Pi]$ with parameter set $\Pi = \{q, p, Q, P\}$ where $q, p \in \mathbb{R}$ and $Q, P \in \mathbb{C}$. Starting from the k-th order state:

$$\begin{aligned}\phi_k(x) = &\left(\pi\varepsilon^2\right)^{-\frac{1}{4}} 2^{-\frac{k}{2}} \left(k!\right)^{-\frac{1}{2}} Q^{-\frac{k+1}{2}} \overline{Q}^{\frac{k}{2}} \cdot H_k\left(\varepsilon^{-1}|Q|^{-1}\left(x-q\right)\right) \\ &\cdot \exp\left(\frac{\imath}{2\varepsilon^2} P Q^{-1}\left(x-q\right)^2 + \frac{\imath}{\varepsilon^2} p\left(x-q\right)\right)\end{aligned} \tag{55}$$

our goal is to find a variable transformation $x \to y$ such that:

$$\phi_k(y) = \left(\varepsilon^2\right)^{-\frac{1}{4}} C_k \, Q_k \, H_k(y) \, \exp\left(-\frac{y^2}{2}\right) R(y) \tag{56}$$

where:

$$C_k := \pi^{-\frac{1}{4}} 2^{-\frac{k}{2}} \left(k!\right)^{-\frac{1}{2}} \quad \text{and} \quad Q_k := Q^{-\frac{k+1}{2}} \overline{Q}^{\frac{k}{2}} \tag{57}$$

and there is some factor $R(y)$ that collects all remaining junk terms. The argument of the Hermite polynomial H_k suggests the transformation:

$$y = \varepsilon^{-1}|Q|^{-1}(x-q) \quad \leftrightarrow \quad x = q + \varepsilon|Q|y \, . \tag{58}$$

Plugging the equality $x - q = \varepsilon|Q|y$ into the exponential part of the formula for ϕ_k we obtain:

$$\begin{aligned}&\exp\left(\frac{\imath}{2\varepsilon^2} P Q^{-1}\left(x-q\right)^2 + \frac{\imath}{\varepsilon^2} p\left(x-q\right)\right) \\ = &\exp\left(\frac{\imath}{2\varepsilon^2} P Q^{-1}\left(\varepsilon|Q|y\right)^2 + \frac{\imath}{\varepsilon^2} p\left(\varepsilon|Q|y\right)\right) \\ = &\exp\left(\frac{\imath}{2} P Q^{-1}|Q|^2 y^2\right) \exp\left(\frac{\imath}{\varepsilon} p|Q|y\right) \, .\end{aligned}$$

Next we use the fact that $|Q|^2 = Q\overline{Q}$ and expand the first term further:

$$\begin{aligned}&= \exp\left(\frac{\imath}{2} P Q^{-1} Q \overline{Q} y^2\right) \exp\left(\frac{\imath}{\varepsilon} p|Q|y\right) \\ &= \exp\left(-\frac{1}{2} y^2 (-\imath P \overline{Q})\right) \exp\left(\frac{\imath}{\varepsilon} p|Q|y\right) \, .\end{aligned}$$

Compared to our goal we got an extra factor $-\imath P\overline{Q} \neq 1$ in the exponential. We decompose the complex parameters $P = P_r + \imath P_i$ and $Q = Q_r + \imath Q_i$ into their real and imaginary parts and stick them into the compatibility formula:

$$\overline{Q}P - \overline{P}Q = 2\imath \tag{59}$$

which yields:

$$\begin{aligned}2\imath &= \left(Q_r - \imath Q_i\right)\left(P_r + \imath P_i\right) - \left(P_r - \imath P_i\right)\left(Q_r + \imath Q_i\right) \\ &= P_r Q_r - \imath P_r Q_i + \imath P_i Q_r + P_i Q_i - P_r Q_r - \imath P_r Q_i + \imath P_i Q_r - P_i Q_i \\ &= 2\imath\left(P_i Q_r - P_r Q_i\right)\end{aligned} \tag{60}$$

from where it follows that $P_iQ_r - P_rQ_i = 1$. Returning to our original factor we start with:

$$\begin{aligned} -\imath P\overline{Q} &= -\imath\left(P_r + \imath P_i\right)\left(Q_r - \imath Q_i\right) \\ &= -\imath\left(P_rQ_r - \imath P_rQ_i + \imath P_iQ_r + P_iQ_i\right) \\ &= P_iQ_r - P_rQ_i - \imath P_rQ_r - \imath P_iQ_i \\ &= 1 - \imath\left(P_rQ_r + P_iQ_i\right) \end{aligned} \tag{61}$$

and split the factor into a unit and $P_rQ_r + P_iQ_i \in \mathbb{R}$. Combining this with the previous result we get:

$$\begin{aligned} &\exp\left(-\frac{1}{2}y^2\left(1 - \imath\left(P_rQ_r + P_iQ_i\right)\right)\right)\exp\left(\frac{\imath}{\varepsilon}p|Q|y\right) \\ &= \exp\left(-\frac{1}{2}y^2\right)\exp\left(\frac{\imath}{2}y^2\left(P_rQ_r + P_iQ_i\right)\right)\exp\left(\frac{\imath}{\varepsilon}p|Q|y\right) \end{aligned}$$

and find:

$$R(y) = \exp\left(\frac{\imath}{2}y^2\left(P_rQ_r + P_iQ_i\right)\right)\exp\left(\frac{\imath}{\varepsilon}p|Q|y\right) \tag{62}$$

and finally:

$$\phi_k(y) = \left(\varepsilon^2\right)^{-\frac{1}{4}} Q_k C_k H_k(y)\exp\left(-\frac{1}{2}y^2\right) R(y) \tag{63}$$

with the factors as defined in (57). It is important to note that the exponentials in $R(y)$ contain purely imaginary arguments which can be seen by the definition of the quantities involved. The y is real valued and so is $|Q| \in \mathbb{R}$ and the real and imaginary parts of Q and P. The importance of this computation lies in the fact that we can replace the middle part $C_kH_k(y)\exp\left(-\frac{1}{2}y^2\right)$ by a Hermite *function* $h_k(y)$ to get:

$$\phi_k(y) = \varepsilon^{-\frac{1}{2}} Q_k\, h_k(y)\, R(y)\,. \tag{64}$$

6.2 Multidimensional case

In the D dimensional case we have a wavepacket $\phi_{\underline{k}}[\Pi]$ with parameter set $\Pi = \{\underline{q}, \underline{p}, \mathbf{Q}, \mathbf{P}\}$ consisting of vectors $\underline{q}, \underline{p} \in \mathbb{R}^D$ and matrices $\mathbf{Q}, \mathbf{P} \in \mathbb{C}^{D\times D}$. The $\underline{k} \in \mathbb{N}_0^D$ is a suitable multi-index. To attack the multidimensional case we claim that the wavepacket can be written like:

$$\begin{aligned} \phi_{\underline{k}}(\underline{x}) = &\left(\pi\varepsilon^2\right)^{-\frac{D}{4}} \det(\mathbf{Q})^{-\frac{1}{2}} \prod_{i=1}^{D} 2^{-\frac{k_i}{2}}\left(\underline{k}_i!\right)^{-\frac{1}{2}} \\ &\cdot H_{\underline{k}}\left(\varepsilon^{-1}|\mathbf{Q}|^{-1}\left(\underline{x} - \underline{q}\right)\right) \\ &\cdot \exp\left(\frac{i}{2\varepsilon^2}\left\langle(\underline{x} - \underline{q}), \mathbf{P}\mathbf{Q}^{-1}(\underline{x} - \underline{q})\right\rangle + \frac{i}{\varepsilon^2}\left\langle \underline{p}, (\underline{x} - \underline{q})\right\rangle\right) \end{aligned} \tag{65}$$

and we define the constant $C_{\underline{k}}$ as:

$$C_{\underline{k}} := \pi^{-\frac{D}{4}} 2^{-\frac{\underline{k}}{2}}\left(\underline{k}!\right)^{-\frac{1}{2}} := \prod_{i=1}^{D} \pi^{-\frac{1}{4}} 2^{-\frac{k_i}{2}}\left(\underline{k}_i!\right)^{-\frac{1}{2}} \tag{66}$$

and the complex constant $Q_{\underline{k}}$ with $Q_{\underline{0}} := \det(\mathbf{Q})^{-\frac{1}{2}}$. Our goal is to find a similar transformation as in the scalar case and by analogy we examine the candidate:

$$\underline{y} = \varepsilon^{-1}|\mathbf{Q}|^{-1}(\underline{x} - \underline{q}) \quad \leftrightarrow \quad \underline{x} = \underline{q} + \varepsilon|\mathbf{Q}|\underline{y}\,. \tag{67}$$

We start again by plugging $\underline{x} - \underline{q} = \varepsilon|\mathbf{Q}|\underline{y}$ into the inner products inside the exponential:

$$\begin{aligned}
&\exp\left(\frac{i}{2\varepsilon^2}\left\langle \underline{x} - \underline{q}, \mathbf{P}\mathbf{Q}^{-1}(\underline{x} - \underline{q})\right\rangle + \frac{i}{\varepsilon^2}\left\langle \underline{p}, \underline{x} - \underline{q}\right\rangle\right) \\
&= \exp\left(\frac{i}{2\varepsilon^2}\left\langle \varepsilon|\mathbf{Q}|\underline{y}, \mathbf{P}\mathbf{Q}^{-1}\varepsilon|\mathbf{Q}|\underline{y}\right\rangle + \frac{i}{\varepsilon^2}\left\langle \underline{p}, \varepsilon|\mathbf{Q}|\underline{y}\right\rangle\right) \\
&= \exp\left(\frac{i}{2}\left\langle |\mathbf{Q}|\underline{y}, \mathbf{P}\mathbf{Q}^{-1}|\mathbf{Q}|\underline{y}\right\rangle\right)\exp\left(\frac{i}{\varepsilon}\left\langle \underline{p}, |\mathbf{Q}|\underline{y}\right\rangle\right)\,.
\end{aligned}$$

Next we use the definition of $|\mathbf{Q}| := (\mathbf{Q}\mathbf{Q}^{\mathrm{H}})^{\frac{1}{2}}$ and concentrate on the main exponential:

$$\begin{aligned}
&\exp\left(\frac{i}{2}\left\langle |\mathbf{Q}|\underline{y}, \mathbf{P}\mathbf{Q}^{-1}|\mathbf{Q}|\underline{y}\right\rangle\right) \\
&= \exp\left(\frac{i}{2}\left\langle \underline{y}, (\mathbf{Q}\mathbf{Q}^{\mathrm{H}})^{\frac{\mathrm{H}}{2}}\mathbf{P}\mathbf{Q}^{-1}(\mathbf{Q}\mathbf{Q}^{\mathrm{H}})^{\frac{1}{2}}\underline{y}\right\rangle\right)
\end{aligned}$$

then we split the central factor as $\mathbf{P}\mathbf{Q}^{-1} = \Re(\mathbf{P}\mathbf{Q}^{-1}) + \imath\Im(\mathbf{P}\mathbf{Q}^{-1})$:

$$\begin{aligned}
&= \exp\left(\frac{i}{2}\left\langle \underline{y}, (\mathbf{Q}\mathbf{Q}^{\mathrm{H}})^{\frac{\mathrm{H}}{2}}\left(\Re(\mathbf{P}\mathbf{Q}^{-1}) + \imath\Im(\mathbf{P}\mathbf{Q}^{-1})\right)(\mathbf{Q}\mathbf{Q}^{\mathrm{H}})^{\frac{1}{2}}\underline{y}\right\rangle\right) \\
&= \exp\left(-\frac{1}{2}\left\langle \underline{y}, (\mathbf{Q}\mathbf{Q}^{\mathrm{H}})^{\frac{\mathrm{H}}{2}}\Im(\mathbf{P}\mathbf{Q}^{-1})(\mathbf{Q}\mathbf{Q}^{\mathrm{H}})^{\frac{1}{2}}\underline{y}\right\rangle\right)\exp\left(\frac{i}{2}\left\langle \underline{y}, (\mathbf{Q}\mathbf{Q}^{\mathrm{H}})^{\frac{\mathrm{H}}{2}}\Re(\mathbf{P}\mathbf{Q}^{-1})(\mathbf{Q}\mathbf{Q}^{\mathrm{H}})^{\frac{1}{2}}\underline{y}\right\rangle\right)
\end{aligned}$$

and in turn take a closer look at the exponential containing the imaginary part. We use the fact that $\Im(\mathbf{P}\mathbf{Q}^{-1}) = (\mathbf{Q}\mathbf{Q}^{\mathrm{H}})^{-1}$ holds where $(\mathbf{Q}\mathbf{Q}^{\mathrm{H}})^{-1}$ is real valued and symmetric positive definite:

$$\begin{aligned}
&\exp\left(-\frac{1}{2}\left\langle \underline{y}, (\mathbf{Q}\mathbf{Q}^{\mathrm{H}})^{\frac{\mathrm{H}}{2}}\Im(\mathbf{P}\mathbf{Q}^{-1})(\mathbf{Q}\mathbf{Q}^{\mathrm{H}})^{\frac{1}{2}}\underline{y}\right\rangle\right) \\
&= \exp\left(-\frac{1}{2}\left\langle \underline{y}, (\mathbf{Q}\mathbf{Q}^{\mathrm{H}})^{\frac{1}{2}}(\mathbf{Q}\mathbf{Q}^{\mathrm{H}})^{-1}(\mathbf{Q}\mathbf{Q}^{\mathrm{H}})^{\frac{1}{2}}\underline{y}\right\rangle\right)\,.
\end{aligned}$$

By the eigen decomposition $\mathbf{Q}\mathbf{Q}^{\mathrm{H}} = \mathbf{T}^{-1}\mathbf{\Lambda}\mathbf{T}$ we have:

$$\begin{aligned}
&= \exp\left(-\frac{1}{2}\left\langle \underline{y}, (\mathbf{T}^{-1}\mathbf{\Lambda}\mathbf{T})^{\frac{1}{2}}(\mathbf{T}^{-1}\mathbf{\Lambda}\mathbf{T})^{-1}(\mathbf{T}^{-1}\mathbf{\Lambda}\mathbf{T})^{\frac{1}{2}}\underline{y}\right\rangle\right) \\
&= \exp\left(-\frac{1}{2}\left\langle \underline{y}, \mathbf{T}^{-1}\mathbf{\Lambda}^{\frac{1}{2}}\mathbf{T}\mathbf{T}^{-1}\mathbf{\Lambda}^{-1}\mathbf{T}\mathbf{T}^{-1}\mathbf{\Lambda}^{\frac{1}{2}}\mathbf{T}\underline{y}\right\rangle\right) \\
&= \exp\left(-\frac{1}{2}\left\langle \underline{y}, \mathbf{T}^{-1}\mathbf{\Lambda}^{\frac{1}{2}}\mathbf{\Lambda}^{-1}\mathbf{\Lambda}^{\frac{1}{2}}\mathbf{T}\underline{y}\right\rangle\right) = \exp\left(-\frac{1}{2}\left\langle \underline{y}, \underline{y}\right\rangle\right)\,.
\end{aligned}$$

What remains is to put together all the pieces from above. We will build the factor $R(\underline{y})$ as in the scalar case. First we argue that the exponential containing

the real part of our decomposition[3] has purely imaginary argument. Using the above relation we have:

$$\begin{aligned} &\exp\left(\frac{i}{2}\left\langle \underline{y}, (\mathbf{Q}\mathbf{Q}^{\mathrm{H}})^{\frac{\mathrm{H}}{2}} \Re(\mathbf{P}\mathbf{Q}^{-1}) (\mathbf{Q}\mathbf{Q}^{\mathrm{H}})^{\frac{1}{2}} \underline{y} \right\rangle\right) \\ = &\exp\left(\frac{i}{2}\left\langle \underline{y}, \Im(\mathbf{P}\mathbf{Q}^{-1})^{-\frac{1}{2}} \Re(\mathbf{P}\mathbf{Q}^{-1}) \Im(\mathbf{P}\mathbf{Q}^{-1})^{-\frac{1}{2}} \underline{y} \right\rangle\right) \end{aligned} \tag{68}$$

where we know that $\Im(\mathbf{P}\mathbf{Q}^{-1})$ is symmetric positive definite and the fact follows. In the end we get for the correction factor:

$$R(\underline{y}) := \exp\left(\frac{i}{2}\left\langle \underline{y}, \Im(\mathbf{P}\mathbf{Q}^{-1})^{-\frac{1}{2}} \Re(\mathbf{P}\mathbf{Q}^{-1}) \Im(\mathbf{P}\mathbf{Q}^{-1})^{-\frac{1}{2}} \underline{y} \right\rangle\right) \exp\left(\frac{i}{\varepsilon}\left\langle \underline{p}, |\mathbf{Q}|\underline{y} \right\rangle\right)$$

and for the wavepacket:

$$\phi_{\underline{k}}(\underline{x}) = \varepsilon^{-\frac{D}{2}} Q_{\underline{k}}\, C_{\underline{k}}\, H_{\underline{k}}\left(\underline{y}\right) \exp\left(-\frac{1}{2}\left\langle \underline{y}, \underline{y} \right\rangle\right) R(\underline{y})\,. \tag{69}$$

It is important to mention that the $H_{\underline{k}}\left(\underline{y}\right)$ is *not* simply a tensor product of univariate Hermite polynomials but a much more complicated object. Although there are various multi-variate and multi-index generalizations of the Hermite polynomials, see for example [26, 25, 36, 9, 5, 6, 8] and the references therein, unfortunately none of these seems to fit our case here. In context of Hagedorn wavepackets, these issues were analyzed in depth in several publications, see Remark 5 and Proposition 7 in [16], Corollary 4.6 and the appendix C in [15] as well as the paper [7]. A generating function of $H_{\underline{k}}\left(\underline{y}\right)$ is provided in [11]. For the purpose of our algorithmic approach presented here, this does not resolve the central issues, namely that we need an asymptotic expansion of the polynomials similar as in the one-dimensional case. Hence the multi-variate case stays open for now. This is not too problematic as at least one index $\underline{k}_i$ must exceed a certain threshold, for example about 150 for the asymptotic expansion to become applicable. In multiple dimensions this would result in really huge basis sets $\mathfrak{K}$ anyway.

7 Evaluation of Wavepackets

By the results of the previous sections we can write an implementation of Hagedorn wavepackets which uses the asymptotic approximation as shown in formula (64) to evaluate the packet ϕ_n for n larger than some threshold value N. A good choice for N lies somewhere in the range $400 < N < 600$ but the exact value is not of big importance.

[3] Note that this formula exactly simplifies to the one-dimensional case. Take complex numbers $Q = Q_r + \imath Q_i$ and $P = P_r + \imath P_i$ and compute:

$$\begin{aligned} \Im\left(\frac{P_r+\imath P_i}{Q_r+\imath Q_i}\right)^{-\frac{1}{2}} \Re\left(\frac{P_r+\imath P_i}{Q_r+\imath Q_i}\right) \Im\left(\frac{P_r+\imath P_i}{Q_r+\imath Q_i}\right)^{-\frac{1}{2}} &= \Im\left(\frac{P_r+\imath P_i}{Q_r+\imath Q_i}\right)^{-1} \Re\left(\frac{P_r+\imath P_i}{Q_r+\imath Q_i}\right) \\ &= \left(\frac{P_iQ_r - P_rQ_i}{Q_r^2+Q_i^2}\right)^{-1} \left(\frac{P_rQ_r+P_iQ_i}{Q_r^2+Q_i^2}\right) \\ &= P_rQ_r + P_iQ_i \end{aligned}$$

It follows from the compatibility relation $\overline{Q}P - \overline{P}Q = 2\imath$ that $P_iQ_r - P_rQ_i = 1$ holds.

First we try to evaluate the lowest order wavepackets $\phi_0, \ldots, \phi_3$, the results are shown in Figure 21. Given the derivation above, this is not expected to give very pleasant results, but it turns out not to be that bad.

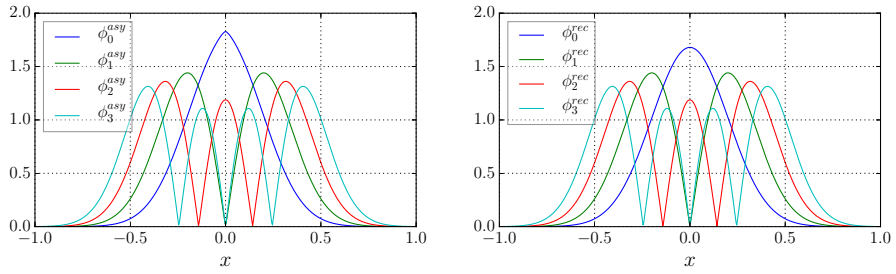

Figure 21: Evaluation of the first 4 wavepackets ϕ_0 to ϕ_4 by asymptotic approximation (left) and recursion (right). The recursion gives the exact solution but also the approximation works surprisingly well. The Gaussian ϕ_0 is too pointed at $x = 0$, but the ϕ_1 already looks quite good.

A more sensible comparison is given in Figure 22 where we compute and plot the point-wise absolute difference $|\phi_n^{asy} - \phi_n^{rec}|$ for several interesting ranges of n. Relative errors $|\phi_n^{asy} - \phi_n^{rec}|/|\phi_n^{rec}|$ are given in Figure 23. These results further hint at the choice of N.
Testing our implementation on the examples shown in the beginning, we obtain the last two figures. Figure 24 shows our matrix $\mathbf{M}$ having no artifacts anymore, compared to the matrix printed in Figure 2. The diagonal and off-diagonal elements are correct as shown in Figure 25. We indeed obtain a clean identity matrix.

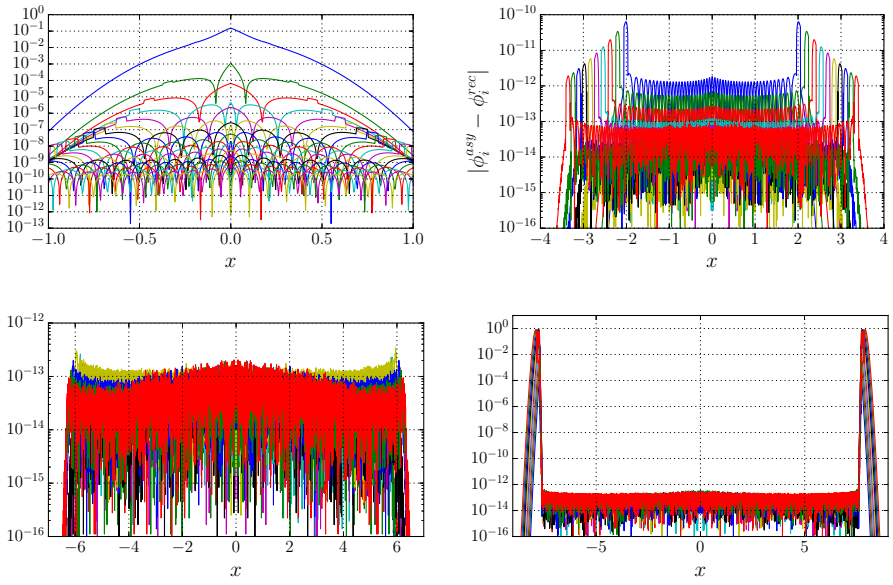

Figure 22: The four plots show the difference $|\phi_n^{asy} - \phi_n^{rec}|$ between the recursive evaluation and the asymptotic approximation of ϕ_n for various values of n. Top left: $0 \leq n < 20$. We see that the maximal point-wise error for ϕ_1 is about 10^{-3} and that this error decreases to 10^{-10} for the following ϕ_n. Top right: n varies in the range 50 to 150 by steps of 10. Except for the borders the error is constant low. However, the n is still to small for a uniformly good approximation. Bottom left: n varies in the range 400 to 500 by steps of 10. In this range the asymptotic approximation does well with errors in the order of 10^{-14}. Bottom right: n varies in the range 700 to 800 by steps of 10. Here we see the break down of the reference ϕ_n^{rec}.

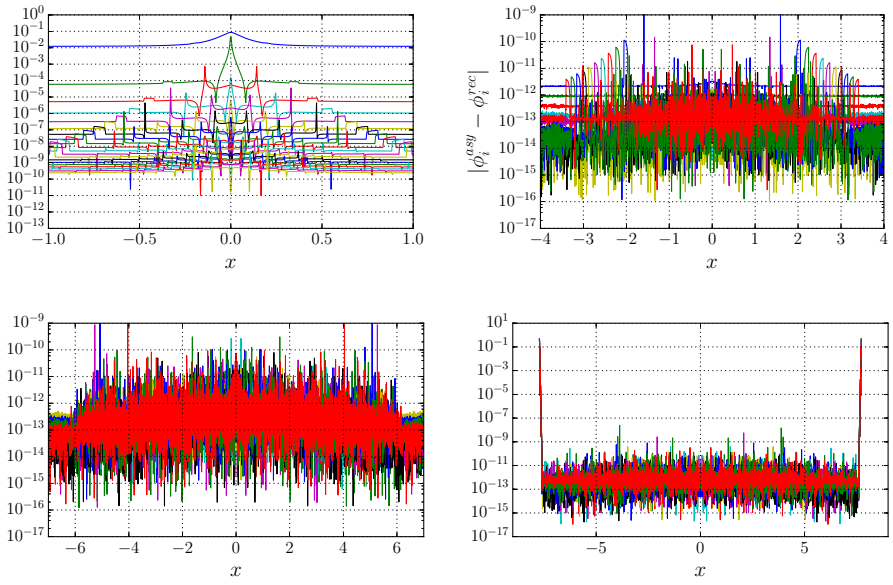

Figure 23: The relative errors $|\phi_n^{asy} - \phi_n^{rec}|/|\phi_n^{rec}|$ instead of the absolute errors as shown in Figure 22.

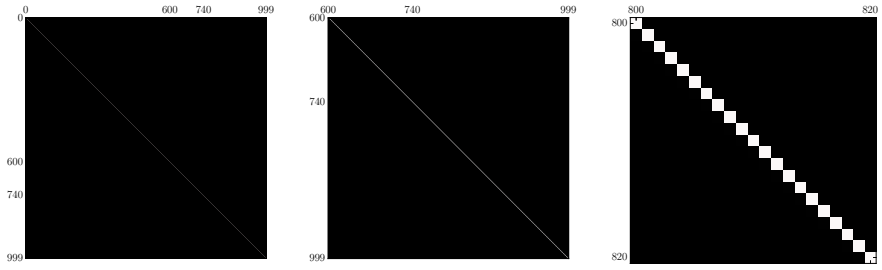

Figure 24: Plot of the overlap matrix $\mathbf{M}_{r,c} := \langle \phi_r | \phi_c \rangle$. We obtain a pure identity matrix without any artifacts when using the asymptotic approximation for high order wavepackets ϕ_n with $n > N$.

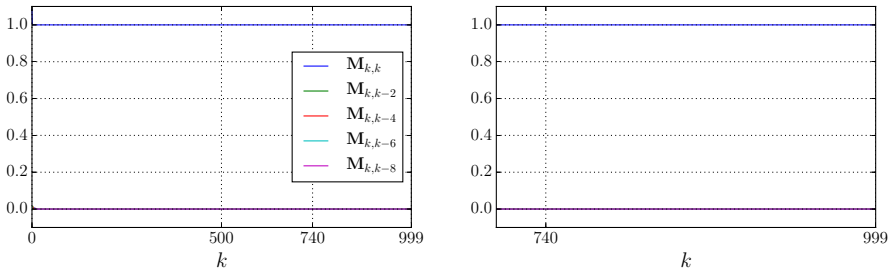

Figure 25: Diagonal and selected off-diagonal elements of the matrix $\mathbf{M}$. Compared to the results in Figure 3 the output matches an identity matrix.

8 Conclusion

Although mathematically stable, the three term recursion for the Hermite functions $h_n(x)$ can fail to give correct function values for a large parameter n. This is caused by the insufficiency of finite floating point arithmetic in combination with the recursion as demonstrated in the beginning.
We presented an alternative method for the evaluation of Hermite functions. Our method, based on well-known powerful but complicated asymptotic expansions in terms of Airy special functions, gives correct function values for medium to large order n and arbitrary (real) argument x. We can even evaluate any single function h_n in constant time independent on the value of n.
However, it should be noted that this algorithm performs more operations compared to the simple recursion and therefore is slower than the recursive approach. In some trivial test case we measured a factor of about 10. Therefore one should use the recursive computation whenever possible. Our approach is favorable mainly under two conditions: the necessity to work with n and x in a range where the recursion fails and the desire to evaluate just a single h_n avoiding the computation of all its precursors. We strive to include this evaluation algorithm into the SciPy library [14].
We employed this algorithm for the construction and evaluation respectively of Hagedorn wavepackets. In the one-dimensional case these wavepackets consist of Hermite functions together with some generally complex scale and shift factors. Hence one can now work with much larger basis sets built of wavepackets. We implemented this algorithmic procedure in the WaveBlocks library [2].
In the multi-dimensional case the same technique unfortunately is not applicable directly. The Hagedorn wavepackets in general do not follow a tensor product structure and hence a decomposition into one-dimensional Hermite functions is not possible, unless expensive transformation steps are performed [12].

References

[1] NIST Digital Library of Mathematical Functions. http://dlmf.nist.gov/, Release 1.0.10 of 2015-08-07. Online companion to [22]. 3, 7, 15, 32

[2] R. Bourquin and V. Gradinaru. WaveBlocks: Reusable building blocks for simulations with semiclassical wavepackets. https://github.com/WaveBlocks/WaveBlocksND, 2010 - 2016. 31

[3] Benjamin F. Bunck. A fast algorithm for evaluation of normalized Hermite functions. *BIT Numerical Mathematics*, 49(2):281–295, 2009. 1

[4] A. B. Olde Daalhuis and N. M. Temme. Uniform Airy-type expansions of integrals. *SIAM Journal on Mathematical Analysis*, 25(2):304–321, 1994. 4

[5] G. Dattoli. Incomplete 2d Hermite polynomials: properties and applications. *Journal of Mathematical Analysis and Applications*, 284(2):447 – 454, 2003. 27

[6] G. Dattoli, S. Lorenzutta, G. Maino, and A. Torre. Theory of multiindex multivariable Bessel functions and Hermite polynomials. *Le Matematiche*, 52(1):179–197, 1998. 27

[7] H. Dietert, J. Keller, and S. Troppmann. An invariant class of wave packets for the Wigner transform. *ArXiv e-prints*, 05 2015. 27

[8] V V Dodonov. Asymptotic formulae for two-variable hermite polynomials. *Journal of Physics A: Mathematical and General*, 27(18):6191, 1994. 27

[9] Allal Ghanmi. A class of generalized complex Hermite polynomials. *Journal of Mathematical Analysis and Applications*, 340(2):1395 – 1406, 2008. 27

[10] A. Gil, J. Segura, and N. Temme. *Numerical Methods for Special Functions*. Society for Industrial and Applied Mathematics, 2007. 4

[11] G. A. Hagedorn. Generating function and a Rodrigues formula for the polynomials in d-dimensional semiclassical wave packets. *Annals of Physics*, 362:603–608, 11 2015. 27

[12] George A. Hagedorn and Caroline Lasser. Symmetric Kronecker products and semiclassical wave packets. *arXiv:1603.04284 [math.NA]*, 2016. 31

[13] D. S. Jones. Parabolic cylinder functions of large order. *J. Comput. Appl. Math.*, 190(1-2):453–469, 2006. 4

[14] Eric Jones, Travis Oliphant, Pearu Peterson, et al. SciPy: Open source scientific tools for Python, 2001–. [Online; accessed 2016-05-23]. 5, 31

[15] C. Lasser, R. Schubert, and S. Troppmann. Non-hermitian propagation of hagedorn wavepackets. *ArXiv e-prints*, 07 2015. 27

[16] Caroline Lasser and Stephanie Troppmann. Hagedorn wavepackets in time-frequency and phase space. *Journal of Fourier Analysis and Applications*, 20(4):679–714, 2014. 27

[17] Cristinel Mortici. A new fast asymptotic series for the gamma function. *The Ramanujan Journal*, 38(3):549–559, 2014. 9

[18] Gergő Nemes. New asymptotic expansion for the gamma function. *Archiv der Mathematik*, 95(2):161–169, 2010. 9

[19] F. W. J. Olver. Uniform asymptotic expansions for Weber parabolic cylinder functions of large orders. *J. Res. Nat. Bur. Standards Sect. B*, 63B:131–169, 1959. 2, 5, 6, 15

[20] F. W. J. Olver. Whittaker functions with both parameters large: Uniform approximations in terms of parabolic cylinder functions. *Proc. Roy. Soc. Edinburgh Sect. A*, 86(3-4):213–234, 1980. 4

[21] F. W. J. Olver. *Asymptotics and Special Functions*. A. K. Peters, 1997. Reprint, with corrections, of original Academic Press edition, 1974. 2

[22] F. W. J. Olver, D. W. Lozier, R. F. Boisvert, and C. W. Clark, editors. *NIST Handbook of Mathematical Functions*. Cambridge University Press, 2010. Print companion to [1]. 31

[23] F.W.J. Olver and R. Wong. *Selected Papers of F.W.J. Olver*. World Scientific, 2000. 2

[24] J. Segura and A. Gil. Parabolic cylinder functions of integer and half-integer orders for non-negative arguments. *Computer Physics Communications*, 115(1):69 – 86, 1998. 4

[25] HSP Shrivastava. Some generating function relations of multiindex Hermite polynomials. *Mathematical and Computational Applications*, 6(3):189, 2001. 27

[26] HSP Shrivastava. Multiindex multivariable Hermite polynomials. *Mathematical and Computational Applications*, 7(2):139, 2002. 27

[27] John L. Spouge. Computation of the gamma, digamma, and trigamma functions. *SIAM Journal on Numerical Analysis*, 31(3):931–944, 1994. 9

[28] G. Taubmann. Parabolic cylinder functions $U(n, x)$ for natural n and positive x. *Computer Physics Communications*, 69(2):415 – 419, 1992. 4

[29] Nico M. Temme. Numerical and asymptotic aspects of parabolic cylinder functions. *Journal of Computational and Applied Mathematics*, 121(1-2):221 – 246, 2000. Numerical analysis in the 20th century, Vol. I, Approximation theory. 4, 16

[30] Nico M. Temme and Raimundas Vidunas. Parabolic cylinder functions: Examples of error bounds for asymptotic expansions. *Analysis and Applications*, 01(03):265–288, 2003. 4

[31] N.M. Temme. Numerical algorithms for uniform Airy-type asymptotic expansions. *Numerical Algorithms*, 15(2):207–225, 1997. 4

[32] A. Townsend, T. Trogdon, and S. Olver. Fast computation of Gauss quadrature nodes and weights on the whole real line. *ArXiv e-prints*, 10 2014. 9

[33] Alex Townsend, Thomas Trogdon, and Sheehan Olver. Fast computation of Gauss quadrature nodes and weights on the whole real line. *IMA Journal of Numerical Analysis*, 36(1):337–358, 2016. 5, 17, 18, 19

[34] O. Vallée and M. Soares. *Airy Functions and Applications to Physics*. Imperial College Press, 2010. 4

[35] Shi Wei. A globally uniform asymptotic expansion of the Hermite polynomials. *Acta Mathematica Scientia*, 28(4):834–842, 2008. 4

[36] A. Wünsche. Hermite and Laguerre 2d polynomials. *Journal of Computational and Applied Mathematics*, 133(1-2):665 – 678, 2001. 5th Int. Symp. on Orthogonal Polynomials, Special Functions and their Applications. 27